1 August 2001

ELSEVIER

Optics Communications 195 (2001) 85–91

OPTICS COMMUNICATIONS

www.elsevier.com/locate/optcom

Wavefront recovery in shearing interferometry with variable magnitude and direction shear

J. Villa [a,*], G. García [b], G. Gómez [a]

[a] *Centro de Ingeniería y Desarrollo Industrial, Av. Playa Pie de la Cuesta #702, Desarrollo Habitacional San Pablo, C.P. 76130, Querétaro, Qro., Mexico*

[b] *Centro de Investigaciones en Óptica, Apartado Postal 1-948, C.P. 37000, León, Gto., Mexico*

Received 21 March 2001; received in revised form 25 April 2001; accepted 21 May 2001

Abstract

We propose a regularization method for estimating the wavefront from shearing interferometric patterns generated in vectorial shearing interferometry. The method considers shearing patterns with variable magnitude and direction displacement. This regularized technique leads a stable solution of the inverse shearing problem and allows the reduction of the wavefront noise. We present the results of this technique applied on synthetic shearing interferograms. © 2001 Published by Elsevier Science B.V.

PACS: 42.30.Rx; 42.87.−d; 07.05.P

Keywords: Regularization; Shearing interferometry

1. Introduction

Recently there has been a growing interest in the fabrication of asymmetric and large diameter optical devices. Asymmetric elements can provide better or unique solution to specific optical design problems. Optical testing for the analysis of optical devices is carried out with diverse type of interferometers. The most commonly used configurations are the Fizeau and Twyman–Green [1], however, these conventional interferometric systems do not satisfy the requirements to test asymmetric or large diameter elements which has increased the need of developing new techniques. On the other hand shearing interferometric systems [1] have been used in order to solve some problems associated to conventional interferometers. Although the information measured with shearing interferometers is not directly the wavefront but its derivative along the shear direction, they can diminish problems of stability and good quality reference components.

The main characteristic of shear interferometers is that the wavefront is compared with itself splitting it into two parts so that it is not necessary a reference wavefront. These type of interferometers are sensitive to the wavefront slope in the shearing direction, that is, the modulating phase of the interferograms is proportional to the derivative

* Corresponding author.

E-mail addresses: jvilla@cidesi.mx (J. Villa), guigator@foton.cio.mx (G. Gómez).

0030-4018/01/$ - see front matter © 2001 Published by Elsevier Science B.V.
PII: S0030-4018(01)01304-9

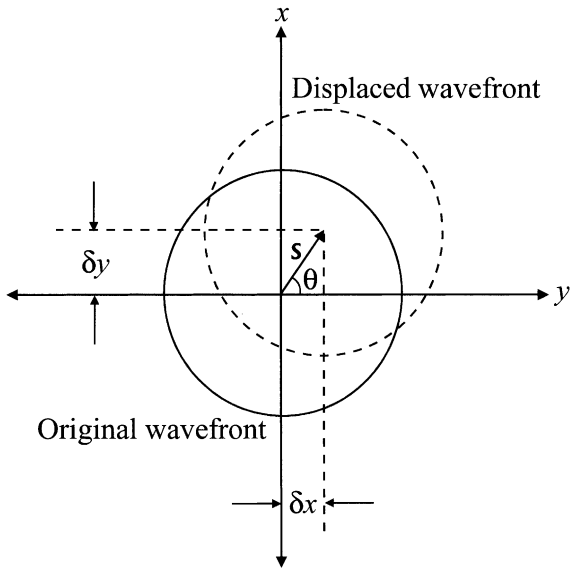

Fig. 1. Schematic diagram of the original and displaced wavefronts in the VSI.

of the wavefront. Other characteristic of shear interferometers is that the sensitivity is controlled by means of the displacement amount that is increased when displacement is increased.

The vectorial shearing interferometer (VSI) [2,3] is a proper alternative to test aspheric and asymmetric optical elements. In the case of the VSI, the wavefront displacement is done along an arbitrary direction, that is, the derivative is directional. Fig. 1 shows the vector displacement in the VSI, where S, θ, δx and δy represent the magnitude, direction, x component, and y component respectively. The advantage of the VSI with respect to traditional lateral shear interferometers [4,5] may be more evident when testing asymmetrical components because in many cases the fringe density in a specific direction is very high [6]. One of the features of this interferometer is the capability of controlling the density and direction of the fringes in the interferograms by a proper selection of wavefront displacement, this is beneficial when asymmetrical components are tested [5].

The objective of shearing interferometers is the recovery of the wavefront from phase differences. Hunt proposed a matrix formulation of phase reconstruction from phase differences [7]. The most common procedure to retrieve the phase from phase derivatives is the least-squares method [8,9]. A more general method that considers directional derivatives in arbitrary directions was proposed by Legarda et al. [10]. These methods, however, assume that the amount of shear is so small that the modulating phase of the shearing interferograms may be considered the wavefront derivative. Servín et al. [11] proposed a regularization method to integrate the wavefront difference fields. This method consists in the improvement of the least-squared method including a regularization term to control the smoothness of the wavefront to be recovered. An advantage of the algorithm with respect to the proposed in Refs. [8,9] is that assumes the amount of shear may be bigger than one pixel. However, this regularization method considers that shearing is performed just along orthogonal directions, x and y.

As we show below, we can retrieve phase from phase differences along arbitrary direction and variable amount of shear. We propose a regularized technique that can be applied even if the sheared interferograms are not mutually orthogonal while keeping good properties of method described in Ref. [11]. The principle of the technique is described in Section 2. Experimental results using synthetic interferograms are presented in Section 3. Finally, conclusions are given in Section 4.

2. Wavefront estimation from sheared phase

An interferogram represents an intensity distribution in the two dimensional space. The interferogram is produced by superimposing two wavefronts where at least one of them is the wavefront shape to be measured. The complex amplitude of the two wavefronts that interfere in a observing plane (e.g. a CCD array) is considered the addition of the complex amplitudes of the two waves [12], that is

$$E(x,y) = A_1(x,y)\exp[\mathrm{i}kW_1(x,y)] + A_2(x,y)\exp[\mathrm{i}kW_2(x,y)]. \quad (1)$$

In Eq. (1) A_1 and A_2 are the amplitudes of the waves, and $k = 2\pi/\lambda$, where λ is the wavelength of the light source and $W_1(x,y)$ and $W_2(x,y)$ represent the shape of the wavefronts interfering. Hence, the irradiance can be modelled as

$$E(x,y)E^*(x,y) = A_1^2(x,y) + A_2^2(x,y) + 2A_1(x,y)A_2(x,y) \times \cos\{k[W_1(x,y) - W_2(x,y)]\}, \quad (2)$$

where the asterisk $(*)$ denotes complex conjugated.

Taking into account that we use a VSI interferometer to test an optical wavefront, we assume that the displacement is performed with an arbitrary magnitude and direction. In this case we call δx_1 and δy_1 the vector components of the displacement along the x- and y-axis respectively. For simplicity, if we consider $A_1 = A_2$, the intensity of the fringe pattern may be expressed as

$$I_1(x,y) = a(x,y) + b(x,y)\cos\{k[W(x,y) - W(x - \delta x_1, y - \delta y_1)]\}, \quad (3)$$

where $a(x,y)$ and $b(x,y)$ represent the background illumination and the amplitude modulation respectively that vary slowly compared with the wavefront $W(x,y)$.

The detected wavefront differences from the interferogram described by Eq. (3) may be represented by

$$\Phi_1(x,y) = [W(x,y) - W(x - \delta x_1, y - \delta y_1)]. \quad (4)$$

Generally, to recover the wavefront from derivatives or differences we need at least two interferograms with different shear direction so that a second wavefront difference field $\Phi_2(x,y)$ recovered from a second interferogram is required. In such circumstances we can integrate the wavefront differences applying the least-squares technique minimizing the cost function

$$U_{\mathrm{LS}} = \sum_{(x,y)\in L} [\widehat{W}(x,y) - \widehat{W}(x - \delta x_1, y - \delta y_1) - \Phi_1(x,y)]^2 + \sum_{(x,y)\in L} [\widehat{W}(x,y) - \widehat{W}(x - \delta x_2, y - \delta y_2) - \Phi_2(x,y)]^2, \quad (5)$$

where L is a finite regular lattice and $\widehat{W}$ is the wavefront to be estimated.

There are two drawbacks using least-squares integration in shear interferometry (see Ref. [11]): (1) The spatial frequency response of the method has zeros at $\omega_v = n\pi/\delta_v$, $n = 0, 1, 2\ldots$, where δ_v represents the displacement in direction v. (2) Least-squares techniques of integration does not provide suitable results because the observations $\Phi_1(x,y)$ and $\Phi_2(x,y)$ do not determine the value of the estimated field $\widehat{W}(x,y)$ in an unique and stable way, that is because least-squares method does not include any information about the nature of the solution, e.g., smoothness of the estimated signal. This is specially important with noisy observations.

Because of the two problems mentioned above, the wavefront recovery from phase differences is an ill-posed problem in the sense of Hadamard [13]. We can alleviate them using regularization theory [14]. In a regularization technique we may include information that restricts the solution to have specific characteristics, e.g., to be smooth. We may include a term in function (5) that corresponds to an a priori assumption of smoothness. If we assume that the estimated field (i.e. $\widehat{W}(x,y)$) has to be globally smooth, the regularization term may consist of a linear combination of squares of discrete approximations to partial derivatives inside the domain of interest [11,14]. With this term we constrain the solution to have smooth derivatives. If we use a discrete approximation to the Laplacian in the regularization term, the cost function is expressed as

$$U_W = U_{\mathrm{LS}} + R, \quad (6)$$

where

$$U_{\mathrm{LS}} = \sum_{(x,y)\in L} \Big[\widehat{W}(x,y) - \widehat{W}(x - \delta x_1, y - \delta y_1) - \Phi_1(x,y)\Big]^2 m(x,y)m(x - \delta x_1, y - \delta y_1) + \sum_{(x,y)\in L} \Big[\widehat{W}(x,y) - \widehat{W}(x - \delta x_2, y - \delta y_2) - \Phi_2(x,y)\Big]^2 m(x,y)m(x - \delta x_2, y - \delta y_2), \quad (7)$$

and

$$R = \mu \sum_{(x,y)\in L} \left[\widehat{W}(x+1,y) - 2\widehat{W}(x,y) + \widehat{W}(x-1,y)\right]^2 \times m(x+1,y)m(x-1,y) + \mu \sum_{(x,y)\in L} \left[\widehat{W}(x,y+1) - 2\widehat{W}(x,y) + \widehat{W}(x,y-1)\right]^2 \times m(x,y+1)m(x,y-1). \quad (8)$$

In Eq. (6) we have included the field $m(x,y)$ that defines the common interference area of the two interferograms. This field is equal to one within this region and zero otherwise. Parameter μ controls the smoothness of the field to be estimated whose value depends on the amount of noise. The bigger the amount of noise the bigger most be the value of this parameter. There is not a precise formula for the determination of this parameter in a given problem so that it is commonly selected intuitively [15]. The minimizer $\widehat{W}$ of Eq. (6) smooths out the observations, hence the minimization operation can also be considered a low-pass filtering operation.

To minimize the cost function U_W we take the gradient with respect to $\widehat{W}(x,y)$ and equating it to zero.

$$\frac{\partial U_W}{\partial \widehat{W}(x,y)} = 2(DU_{\mathrm{LS}} + DR) = 0, \quad (9)$$

where

$$\begin{aligned} DU_{\mathrm{LS}} = {} & [\widehat{W}(x,y) - \widehat{W}(x-\delta x_1, y-\delta y_1) - \Phi_1(x,y)] \\ & \times m(x,y)m(x-\delta x_1, y-\delta y_1) \\ & - [\widehat{W}(x+\delta x_1, y+\delta y_1) - \widehat{W}(x,y) \\ & \quad - \Phi_1(x+\delta x_1, y+\delta y_1)] \\ & \times m(x,y)m(x+\delta x_1, y+\delta y_1) \\ & + [\widehat{W}(x,y) - \widehat{W}(x-\delta x_2, y-\delta y_2) \\ & \quad - \Phi_2(x,y)]m(x,y)m(x-\delta x_2, y-\delta y_2) \\ & - [\widehat{W}(x+\delta x_2, y+\delta y_2) - \widehat{W}(x,y) \\ & \quad - \Phi_2(x+\delta x_2, y+\delta y_2)] \\ & \times m(x,y)m(x+\delta x_2, y+\delta y_2), \end{aligned} \quad (10)$$

and

$$\begin{aligned} DR = {} & \mu[\widehat{W}(x,y) - 2\widehat{W}(x-1,y) + \widehat{W}(x-2,y)] \\ & \times m(x,y)m(x-2,y) - 2\mu[\widehat{W}(x+1,y) \\ & \quad - 2\widehat{W}(x,y) + \widehat{W}(x-1,y)]m(x+1,y) \\ & \times m(x-1,y) + \mu[\widehat{W}(x+2,y) - 2\widehat{W}(x+1,y) \\ & \quad + \widehat{W}(x,y)]m(x+2,y)m(x,y) + \mu[\widehat{W}(x,y) \\ & \quad - 2\widehat{W}(x,y-1) + \widehat{W}(x,y-2)] \\ & \times m(x,y)m(x,y-2) - 2\mu[\widehat{W}(x,y+1) \\ & \quad - 2\widehat{W}(x,y) + \widehat{W}(x,y-1)] \\ & \times m(x,y+1)m(x,y-1) + \mu[\widehat{W}(x,y+2) \\ & \quad - 2\widehat{W}(x,y+1) + \widehat{W}(x,y)] \\ & \times m(x,y+2)m(x,y). \end{aligned} \quad (11)$$

The solution $\widehat{W}(x,y)$ of the linear system (9) may be obtained by using any iterative technique from the literature [16,17]. In our experiments we applied the Gauss–Seidel method.

The amount of shear S and vector components indicated in Fig. 1 are, in general, real numbers. However, in our algorithm we assume that vector components are integers because of the discrete array of pixels. Following a similar reasoning that in Ref. [11], to overcome this problem we may use the closest integer numbers to the vector components of the shearing, then, we can used the following approximation to the observations:

$$\begin{aligned} \tilde{\Phi}_1(x,y) &= \frac{\sqrt{(\tilde{\delta}x_1)^2 + (\tilde{\delta}y_1)^2}}{\sqrt{\delta x_1^2 + \delta y_1^2}} \Phi_1(x,y), \\ \tilde{\Phi}_2(x,y) &= \frac{\sqrt{(\tilde{\delta}x_2)^2 + (\tilde{\delta}y_2)^2}}{\sqrt{\delta x_2^2 + \delta y_2^2}} \Phi_2(x,y), \end{aligned} \quad (12)$$

where

$$\begin{aligned} \tilde{\delta}x_1 &= \mathrm{int}(\delta x_1 + 0.5), \quad \tilde{\delta}y_1 = \mathrm{int}(\delta y_1 + 0.5), \\ \tilde{\delta}x_2 &= \mathrm{int}(\delta x_2 + 0.5), \quad \tilde{\delta}y_2 = \mathrm{int}(\delta y_2 + 0.5). \end{aligned} \quad (13)$$

With this assumption we minimize Eq. (6) using $\tilde{\Phi}_1(x,y)$, $\tilde{\Phi}_2(x,y)$, $\tilde{\delta}x_1$, $\tilde{\delta}y_1$, $\tilde{\delta}x_2$ and $\tilde{\delta}y_2$. The error caused for this approximation has been negligible in our experiments especially for large displacements and big size grids.

3. Numerical simulations

We have made the following numerical simulations to show the performance of the technique proposed in this paper. Fig. 2(a) and (b) represent two noisy shearing interferograms in two different directions obtained simulating a wavefront described by

$$W(x,y) = 0.06y(x^2+y^2) + 0.04x(x^2+y^2) + 0.0006(x^2+3y^2) + 0.0008(3x^2+y^2), \tag{14}$$

where x and y range from -0.05 to 0.05 m that represents a 0.1×0.1 m image. The value of λ in the experiments was 633 nm. In the current example, the values for the displacement (in pixels) were $\delta x_1 = 4.1$, $\delta y_1 = 7.05$, $\delta x_2 = 8.1$ and $\delta y_2 = -3.0$. The shearograms were processed in a rectangular grid of 200×200 pixels with 256 gray levels.

We applied the technique of Ref. [18] to demodulate the shearing interferograms. The phase recovered from shearograms of Fig. 2(a) and (b) are shown in Fig. 3(a) and (b) respectively.

Fig. 4(a) shows the phase associated to the wavefront under test, integrating with the least-squares technique (i.e., minimizing Eq. (5)). Applying our technique of integration we obtained the results shown in Fig. 4(b). In our experiments, we found (with a try-and-error succession) that best results were obtained using values of μ between 0.1 and 0.3 depending on the amount of noise, for this example we used 0.2. Results show

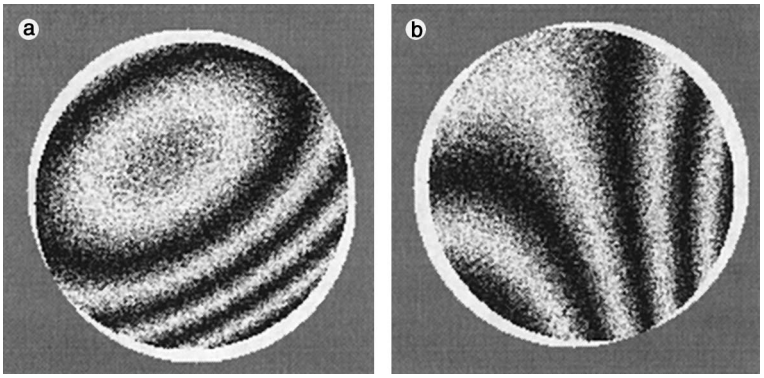

Fig. 2. Synthetic sheared interferograms generated with the wavefront described by Eq. (14) and two different shear directions.

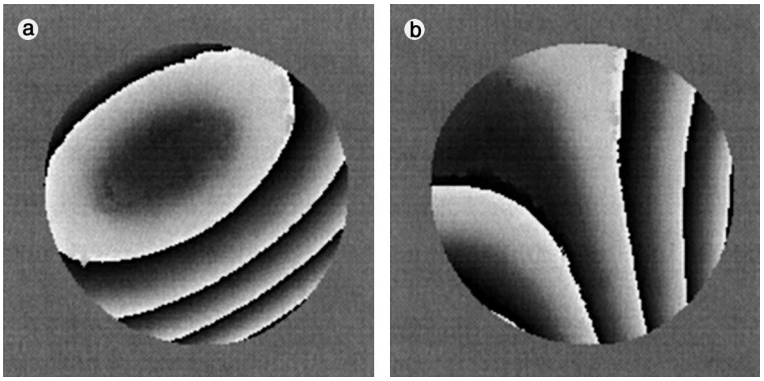

Fig. 3. Phase fields (a) and (b) recovered from interferograms shown in Fig. 2(a) and (b) respectively (shown wrapped).

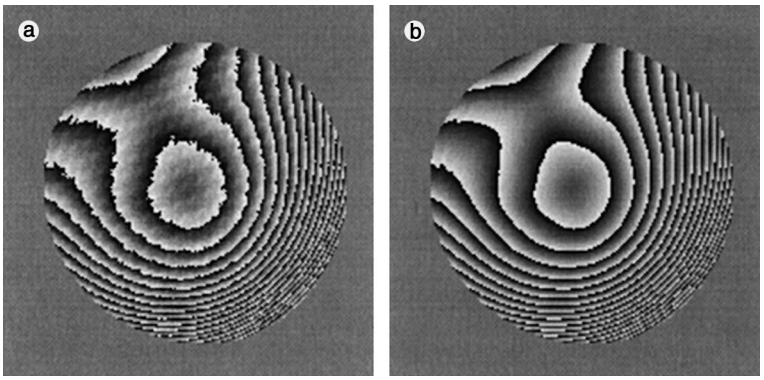

Fig. 4. Associated phase to the wavefront under test recovered with (a) the least-squares technique, and (b) with the proposed technique (shown wrapped). The normalized RMS error were 0.2485 and 0.0562 with the least-squares technique and the proposed technique respectively.

an obvious difference between both techniques. The normalized RMS errors of the phase associated to the wavefront recovered were 0.0562 and 0.2485 with our technique and the least-squares method respectively.

4. Conclusions

We have proposed a technique for integrating the phase differences in arbitrary direction which can be applied to VSI. The novelty of the method is that assembles two possibilities for the shearing: arbitrary direction and variable displacement amount. Our technique also permits the reduction of the wavefront noise and a stable solution of the inverse shearing problem in a controlled way by means of the regularizing parameter. Moreover, the integration of phase differences by means of this technique can be carried out even if the sheared interferograms are not mutually orthogonal. Also it can be applied for other optical tests such as Moiré deflectometry.

Acknowledgements

We acknowledge the support of the Consejo Nacional de Ciencia y Tecnología, México.

References

[1] D. Malacara, Optical Shop Testing, Wiley, New York, 1992.
[2] M. Strojnik, G. García, G. Paez, Vectorial shearing interferometer, SPIE Proc. 3744 (1999) 529–539.
[3] G. Paez, M. Strojnik, G. García, Vectorial shearing interferometer, Appl. Opt. 39 (2000) 5172–5178.
[4] A. Lohmann, O. Bryngdahl, A lateral wave-front shearing interferometer with variable shear, Appl. Opt. 6 (1967) 1934–1937.
[5] M.P. Rimmer, J.C. Wyant, Evaluation of large aberrations using a lateral shear interferometer having variable shear, Appl. Opt. 14 (1975) 142–150.
[6] G. Paez, M. Strojnik, Fringe analysis and phase reconstruction from modulated intensity patterns, Opt. Lett. 22 (1997) 1669–1671.
[7] B.R. Hunt, Matrix formulation of the reconstruction of phase values from phase differences, J. Opt. Soc. Am. 69 (1979) 393–399.
[8] D.L. Fried, Least-squares fitting a wave front distortion estimate to an array of phase difference measurements, J. Opt. Soc. Am. 67 (1977) 370–375.
[9] R.H. Hudgin, Wave-front reconstruction for compensated imaging, J. Opt. Soc. Am. 67 (1977) 375–378.
[10] R. Legarda, M. Rivera, R. Rodríguez, G. Trujillo, Robust wave-front estimation from multiple directional derivatives, Opt. Lett. 25 (2000) 1089–1091.
[11] M. Servín, D. Malacara, J.L. Marroquín, Wave-front recovery from two orthogonal sheared interferograms, Appl. Opt. 35 (1996) 4343–4348.
[12] D. Malacara, M. Servín, Z. Malacara, Interferogram Analysis for optical Testing, Marcel Dekker Inc., 1998.
[13] J. Hadamard, Sur les problems aux derives partielles et leur signification physique, Princeton University Bulletin 13, Princeton University, Princeton, N.J., 1902.

[14] A.N. Thikonov, Solution of incorrectly formulated problems and the regularization method, Sov. Math Dokl. 4 (1963) 1035–1038.
[15] M. Bertero, P. Boccacci, Introduction to Inverse Problems in Imaging, Institute of Physics, London, 1998 (Chapter 5).
[16] G.H. Gollub, C.F. Van Loan, Matrix Computations, Johns Hopkins U. Press, Baltimore, Md., 1990.
[17] R.L. Burden, J.D. Faires, Numerical Analysis, sixth ed., International Thompson Publishing, Stamford, Conn., 1997.
[18] M. Servín, J.L. Marroquín, F.J. Cuevas, Demodulation of a single interferogram by use of a two-dimensional regularized phase-tracking technique, Appl. Opt. 36 (1997) 4540–4548.